Conference paper

Pedro Horta, Marta S. C. Henriques, Elisa M. Brás, Fernanda Murtinheira, Fátima Nogueira, Paul M. O'Neill, José A. Paixão, Rui Fausto and Maria L. S. Cristiano*

On the ordeal of quinolone preparation via cyclisation of aryl-enamines; synthesis and structure of ethyl 6-methyl-7-iodo-4-(3-iodo-4-methylphenoxy)-quinoline-3-carboxylate

DOI 10.1515/pac-2016-1119

Abstract: Recent studies directed to the design of compounds targeting the bc_1 protein complex of *Plasmodium falciparum*, the parasite responsible for most lethal cases of malaria, identified quinolones (4-oxo-quinolines) with low nanomolar inhibitory activity against both the enzyme and infected erythrocytes. The 4-oxo-quinoline 3-ester chemotype emerged as a possible source of potent bc_1 inhibitors, prompting us to expand the library of available analogs for SAR studies and subsequent lead optimization. We now report the synthesis and structural characterization of unexpected ethyl 6-methyl-7-iodo-4-(3-iodo-4-methylphenoxy)-quinoline-3-carboxylate, a 4-aryloxy-quinoline 3-ester formed during attempted preparation of 6-methyl-7-iodo-4-oxo-quinoline-3-carboxylate (4-oxo-quinoline 3-ester). We propose that the 4-aryloxy-quinoline 3-ester derives from 6-methyl-7-iodo-4-hydroxy-quinoline-3-carboxylate (4-hydroxy-quinoline 3-ester), the enol form of 6-methyl-7-iodo-4-oxo-quinoline-3-carboxylate. Formation of the 4-aryloxy-quinoline 3-ester confirms the impact of quinolone/hydroxyquinoline tautomerism, both on the efficiency of synthetic routes to quinolones and on pharmacologic profiles. Tautomers exhibit different cLogP values and interact differently with the enzyme active site. A structural investigation of 6-methyl-7-iodo-4-oxo-quinoline-3-carboxylate and 6-methyl-7-iodo-4-hydroxy-quinoline-3-carboxylate, using matrix isolation coupled to FTIR spectroscopy and theoretical calculations, revealed that the lowest energy conformers of 6-methyl-7-iodo-4-hydroxy-quinoline-3-carboxylate, lower in energy than their most stable 4-oxo-quinoline tautomer by about 27 kJ mol^{-1}, are solely present in the matrix, while the most stable 4-oxo-quinoline tautomer is solely present in the crystalline phase.

Article note: A collection of invited papers based on presentations at the 23rd IUPAC Conference on Physical Organic Chemistry (ICPOC-23), Sydney, Australia, 3–8 July 2016.

***Corresponding author: Maria L. S. Cristiano,** CCMAR and Department of Chemistry and Pharmacy, F.C.T., University of Algarve, P-8005-039 Faro, Portugal, e-mail: mcristi@ualg.pt

Pedro Horta: CCMAR and Department of Chemistry and Pharmacy, F.C.T., University of Algarve, P-8005-039 Faro, Portugal; and Department of Chemistry, University of Liverpool, Liverpool L69 7ZD, UK

Marta S. C. Henriques and José A. Paixão: CFisUC, Department of Physics, University of Coimbra, P-3004-516 Coimbra, Portugal

Elisa M. Brás and Rui Fausto: CQC, Department of Chemistry, University of Coimbra, P-3004-535 Coimbra, Portugal

Fernanda Murtinheira and Fátima Nogueira: CMDT and Institute of Hygiene and Tropical Medicine, New University of Lisbon, P-1349-008 Lisboa, Portugal

Paul M. O'Neill: Department of Chemistry, University of Liverpool, Liverpool L69 7ZD, UK

Keywords: antimalarial activity; ICPOC-23; quinoline 4-ethers; quinolone-hydroxyquinoline tautomerism; quinoline-type *P. falciparum bc*1 complex inhibitors; structural studies; synthesis of quinolones.

Introduction

Quinolines attracted intense research for many decades and, among many achievements, this fruitful effort yielded quinoline-derived drugs that were widely used for the treatment of infections caused by bacteria and parasites [1, 2]. The approval of nalidixic acid as antibacterial drug in 1963 directed researchers to the study of quinolones (oxo-quinolines) [3, 4]. Since then, new medicinal applications of quinolones were unraveled, including for fighting malaria [5].

Malaria remains one of the most deadly infectious diseases in the world. The World Health Organization (WHO) places more than 40 % of the global population at risk of infection by *Plasmodium falciparum*, the most virulent strain among plasmodial pathogens [6]. The growing emergence of resistance by *Plasmodium* parasites against antimalarials in use (including artemisinin-based combinations, ACT's, recommended by WHO) calls for the urgent development of effective antimalarial drugs, preferably directed to new plasmodial targets.

With the approval of Malarone®, a combination of atovaquone and proguanil, for the treatment of malaria, the *P. falciparum* bc_1 protein complex emerged as a suitable target for antimalarial drug design and development. The bc_1 complex is involved in the *Plasmodium* mitochondrial electron transfer chain, an instrumental process in the biosynthetic pathways leading to formation of pyrimidines and ATP [7, 8]. Inhibition of bc_1 leads to a drop of mitochondrial function, collapse of the trans-membrane electrochemical potential and, ultimately, parasite death [9].

Research directed to the design of compounds targeting the bc_1 protein complex identified the quinolone (4-oxo-quinoline) chemotype **1** (Fig. 1) as a possible source of potent inhibitors. Selected quinolones expressed inhibitory activity against the bc_1 protein complex, and also in vitro against infected erythrocytes, at low nanomolar concentrations [5], and subsequent in silico docking studies using the yeast bc_1 suggested that the N–H and the 4-oxo groups play a relevant role in providing antiplasmodial activity [5]. However, differences in activity among members of the original library of compounds **1** were often difficult to interpret, these difficulties being ascribed to the poor solubility (poor pharmacokinetic profile) of quinolones.

Considering the potential demonstrated by the chemotype **1** for developing safe and effective antimalarial drugs, we proposed to expand the library of compounds available for testing, in view of selecting leads with optimized properties. Based on previous in vitro data [5], it was considered that the pharmacologic profile could be tuned by adjusting the nature of substituents at positions 6 and/or 7 of the quinoline core. We thus proposed the synthesis of new 4-oxo-quinoline 3-esters **1** bearing chemical diversity at those positions. To this goal, 4-oxo-quinoline **3** (Scheme 1) was selected as a versatile intermediate, since the 7-iodo substituent can easily be replaced using well established coupling methodologies.

Synthetic routes to compound **3**, depicted in Scheme 1, follow two common methodologies for the preparation of quinolones, described in the literature [10, 11]. Both involve the cyclisation of an enamine

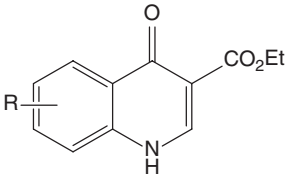

4-Oxo-quinoline (**1**)

Fig. 1: General structure for 4-oxo-quinoline 3-esters investigated.

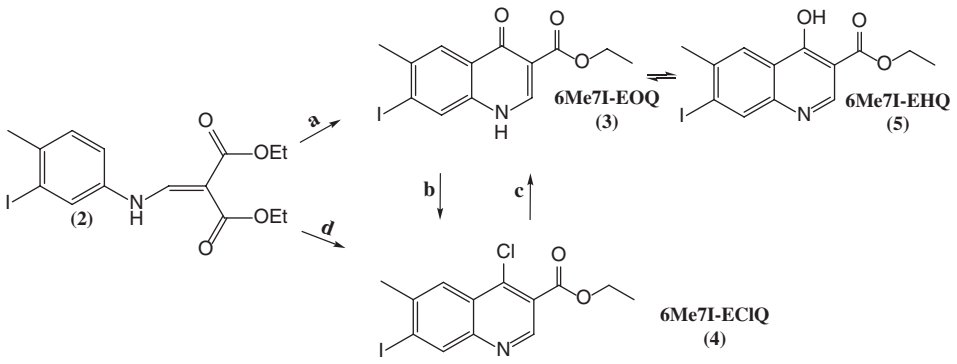

Scheme 1: Synthetic approach to ethyl 6-methyl-7-iodo-4-oxo-quinoline-3-carboxylate (**6Me7I-EOQ, 3**) and to 4-chloro-quinoline (**6Me7I-EClQ, 4**). Conditions: (a) Dowtherm A, 250 °C, 3 h; (b) $POCl_3$, 97 °C, overnight; (c) DMF, HCO_2H/EtOH (80/20), 145 °C, 18 h; (d) $POCl_3$, 97 °C, overnight.

derivative of aniline (the α,β-unsaturated ester derivative **2**), either by heating the enamine in Dowtherm A (at around 250 °C; Gould-Jacobs methodology; route a) or in the presence of $POCl_3$ (at around 100 °C). In this case the process may occur via intermediate formation of 4-chloro-quinoline (**4**; Scheme 1; route d), as previously disclosed [12]. Additionally, 4-chloro-quinoline **4** may be formed from quinolone **3** (Scheme 1; route b), which in turn may isomerise to its 4-hydroxy-tautomer **5** [13]. Thus, the fate of these reactions appears to be quite uncertain and, often, the required quinolones are obtained in poor yields. Optimization of these synthetic procedures requires a better understanding of the reactions involved, the detailed structural analysis of desired products and the identification of by-products formed being relevant to this goal.

In this manuscript we report the isolation and structural characterization of ethyl 6-methyl-7-iodo-4-(3-iodo-4-methylphenoxy)-quinoline-3-carboxylate (**6**; Scheme 2), a 4-phenoxy-quinoline 3-ester formed during attempted preparation of 4-oxo-quinoline **3** *via* route d (Scheme 1). We propose that the 4-aryloxy-quinoline **6** derives from 4-hydroxy-quinoline **5**, the enol form of 4-oxo-quinoline **3** (Scheme 2). The formation of 4-aryloxy-quinoline **6** adds further evidence to the relevance of the quinolone/hydroxyquinoline tautomerism previously described for quinolone 3-esters [13]. This tautomerization impacts in reaction yields and may also impact in the pharmacologic profile of the isolated quinolones. A detailed structural investigation of 4-oxo-quinoline **3** and its tautomer, 4-hydroxy-quinoline **5**, accounting for tautomeric and conformational preferences and relative energies, was undertaken, using matrix isolation coupled to FTIR spectroscopy and quantum chemical calculations.

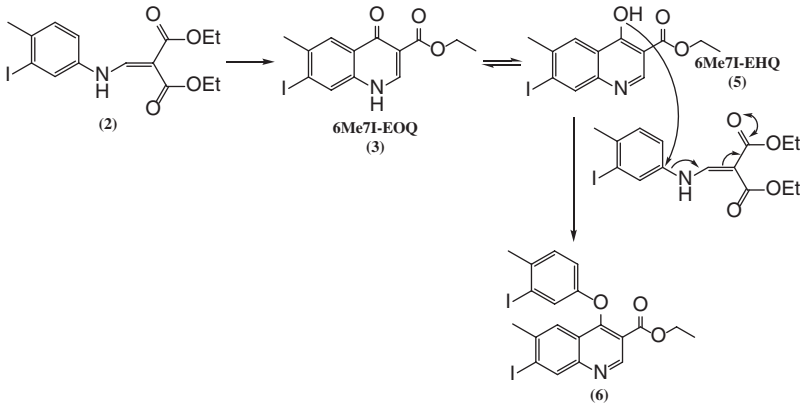

Scheme 2: Schematic representation of the mechanism proposed for the synthesis of 7-iodo-4-(3-iodo-4-methylphenoxy)-6-methyl-quinoline-3-carboxylate **6**.

Experimental section

Synthesis

General methods

All chemicals were used as purchased from commercial sources. Reactions were monitored by TLC, using silica gel F254 plates and a suitable eluent. Inorganic solids were removed by filtration, through a layer of Celite® 512 medium. NMR spectra were measured in appropriate deuterated solvents, using TMS as the internal reference ($\delta = 0.0$ ppm). Chemical shifts (δ) are described in parts per million (ppm). Splitting patterns are designated as *s* (singlet), *d* (doublet), *t* (triplet), *q* (quartet) and *m* (multiplet). NMR spectra for target compounds, operated at 400 and 101 MHz, for ^{1}H and ^{13}C, respectively, are included as supplementary material (Fig. S2, S3, S5, S6, S9 and S10 and Table S1). Mass spectra were recorded via electrospray (ES) or chemical ionization (CI), and are also provided as Supplementary Data (Fig. S1, S4, S7 and S8). Melting points (uncorrected) were recorded on a Stuart Scientific SMP3 melting point apparatus.

Preparation of 3-iodo-4-methylaniline: 2-Iodo-4-nitrotoluene (4 g; 15.2 mmol) was dissolved in a mixture of methanol and water (1 : 1; 30 mL). Ammonium chloride (5.45 g; 101.9 mmol; 6.7 equiv.) and iron powder (3.57 g; 63.9 mmol; 4.2 equiv.) were added and the resulting mixture was stirred vigorously at 60 °C for 4 h. The reaction mixture was cooled, then diluted with methanol and filtered through Celite®. The filtrate was concentrated by evaporation under reduced pressure and the aqueous residue was extracted with ethyl acetate. The combined organic extracts were dried over anhydrous $MgSO_4$, filtered and evaporated to dryness, to give a solid that was recrystallized in ethanol, affording yellow crystals of 3-iodo-4-methylaniline (3.18 g; 90 % yield).

Melting range: 38–40 °C; ^{1}H NMR (400 MHz, D_6-$(CD_3)_2SO$): δ 7.06 (*s*, 1H), 6.92 (*d*, 1H), 6.49 (*d*, 1H), 5.06 (*s*, 2H), 2.17 (*s*, 3H); ^{13}C NMR (101 MHz, D_6-$(CD_3)_2SO$): δ 147.9, 129.8, 126.6, 123.3, 114.2, 101.4, 26.1.; MS (CI+): m/z 234.0 $(M+H)^+$.

Preparation of diethyl 2-((3-iodo-4-methylaniline)methylene)malonate (2): 3-Iodo-4-methylaniline (3 g; 12.9 mmol) and diethyl ethoxymethylenemalonate (2.6 mL; 12.9 mmol) were stirred at 100 °C, overnight. The reaction mixture was cooled and the solid formed was recrystallized in ethanol to give colorless crystals of diethyl 2-((3-iodo-4-methylaniline)methylene)malonate **2** (4.73 g; 91 % yield).

Melting range: 119–121 °C; ^{1}H NMR (400 MHz, $(CD_3)_2SO$): δ 8.30 (*s*, 1H), 7.86 (*s*, 1H), 7.31 (*s*, 2H), 4.15 (*m*, 4H), 2.32 (*s*, 3H), 1.23 (*m*, 6H); ^{13}C NMR (101 MHz, $(CD_3)_2SO$): δ 167.6, 165.6, 151.4, 138.8, 137.5, 130.9, 127.9, 117.9, 102.0, 94.0, 60.3, 60.1, 27.1, 14.7, 14.6.; MS (GC-TOF, EI+): m/z 403.0353 ([M]+).

Preparation of ethyl 4-oxo-6-methyl-7-iodo-quinoline-3-carboxylate (3): Diethyl 2-((3-iodo-4-methylaniline)methylene)malonate **2** (1 g; 2.5 mmol) was suspended in Dowtherm A (10 mL), under a nitrogen atmosphere. The mixture was heated at 250 °C for 3 h and then cooled to room temperature. The solid precipitate was filtered, washed with hexane and diethyl ether and dried, to afford ethyl 4-oxo-6-methyl-7-iodo-quinoline-3-carboxylate **3** as colorless powder (0.55 g; 62 %).

Melting range: 316–317 °C; ^{1}H NMR and ^{13}C NMR data could not be obtained due to insolubility in all available deuterated solvents ($CDCl_3$, $(CD_3)_2SO$, MeOD, D_2O); MS (ES+): m/z 358 $(M+H)^+$, 380 $(M+Na)^+$; Acc Mass: Found 379.9755, calculated 379.9760 for $C_{13}H_{12}INO_3Na$; CHN for $C_{13}H_{12}INO_3$ requires C 43.72 %, H 3.39 %, N 3.92 %, found C 43.67 %, H 3.30 %, N 3.73 %. Detailed structural and vibrational data (both theoretical and experimental), for this compound and for its enol form, 4-hydroxy-quinoline **5**, will be presented and discussed in detail in this article. 4-hydroxy-quinoline **5** could be produced upon sublimation of **6** under high-vacuum, and was studied in both the low temperature (15 K) neat condensed amorphous phase and isolated in an argon matrix.

Preparation of ethyl 7-iodo-4-(3-iodo-4-methylphenoxy)-6-methylquinoline-3-carboxylate (6): Diethyl 2-((3-iodo-4-methylaniline)methylene)malonate **2** (2 g; 5.0 mmol) was suspended in phosphoryl chloride (15 mL), under a nitrogen atmosphere, and the resulting mixture was refluxed overnight at 97 °C. The excess of phosphoryl chloride was removed by distillation under reduced pressure. The resulting residue was cooled to 90 °C and diluted with isopropanol. The final mixture was left to cool slowly and the yellow precipitate was filtered, washed with cold isopropanol and then with cold light petroleum ether. Crystallization from a mixture of DCM and acetone afforded ethyl 7-iodo-4-(3-iodo-4-methylphenoxy)-6-methylquinoline-3-carboxylate **6** (0.35 g; 12% yield). Melting range: 216–218 °C; ^{1}H NMR (400 MHz, $(CD_3)_2SO$): δ 8.87 (*s*, 1H), 8.60 (*s*, 1H), 8.57 (*s*, 1H), 7.73 (*s*, 1H), 7.36 (*d*, 1H), 7.21 (*d*, 1H), 3.76 (*q*, 2H), 2.53 (*s*, 3H), 2.37 (*s*, 3H), 1.10 (*t*, 3H); ^{13}C NMR (101 MHz, $(CD_3)_2SO$): δ 167.0, 164.4, 151.3, 146.7, 139.9, 139.2, 138.3, 131.3, 130.0, 128.6, 123.5, 119.3, 109.2, 107.7, 101.1, 61.5, 27.6, 26.8, 13.7; MS (ES+): m/z 573; Acc Mass: Found 572.9537, calculated 572.9536 for $C_{20}H_{17}NO_3I_2$. Compound **6** was also characterized in the crystalline phase, by X-ray crystallography.

X-ray diffraction studies

X-ray diffraction data for compound **6** were collected at room temperature, using a small single crystal, on a Bruker APEX II diffractometer with graphite monochromatized Mo Kα radiation ($\lambda = 0.71073$ Å). The single-crystal specimen was needle-shaped with dimensions $0.42 \times 0.09 \times 0.07$ mm^3. A monoclinic unit cell [$a = 4.4835(1)$, $b = 18.4261(3)$, $c = 24.6676(4)$ Å, $\beta = 99.731(1)°$] was first derived from indexing the Bragg spots of the first 36 CCD frames and it was further refined by least-squares from the positions of 7814 measured Bragg spots at the end of the data-collection. Systematic absences pointed to the monoclinic $P2_1/c$ space-group, and this assignment was confirmed from the structure solution. Data reduction and a multi-scan absorption correction were performed with the SAINT and SADABS [14] suite of programs.

The crystallographic structure was solved by direct methods using SHELXT-2014/4 [15]. Refinements were carried out with the SHELXL-2014/7 package [16]. All refinements were made by full-matrix least-squares on F^2 with anisotropic displacement parameters for all non-hydrogen atoms. Hydrogen atoms were placed at calculated idealized positions and refined as riding using SHELXL-2014/7 default parameters. The final refinement showed a significant positive residual density of 2.76 e/Å^3 at position (0.0018, 0.3795, 0.0119) that was interpreted as due to an alternate position of the I2 atom of a minor rotational disorder of the 3-iodo-4-methylphenoxy group around the single C–O bonds. Accordingly, the position of the I2 atom was split into the two alternate positions and refined with site occupancies constrained to a sum of one for the two positions.

The refined structural model gave a final R_1 factor of 0.0435 for 3276 reflections of $I > 2\sigma$ and R_{all} of 0.0699 for all 4607 reflections and 243 parameters.

Crystallographic data for the structure in this paper have been deposited with the Cambridge Crystallographic Data Centre as supplementary publication no. CCDC 1495502. Copies of the data can be obtained, free of charge, on application to CCDC, 12 Union Road, Cambridge CB2 1EZ, UK, (fax: +44-(0)1223-336033 or e-mail: deposit@ccdc.cam.ac.Uk).

Infrared spectroscopy studies

The vibrational spectroscopy studies performed were centred on the characterization of the 6-methyl-7-iodo-4-oxo-quinoline-3-carboxylate **3** and its enol form, 6-methyl-7-iodo-4-hydroxy-quinoline-3-carboxylate **5**. The room temperature infrared spectrum of **3** was obtained using the attenuated total reflection technique, with 1 cm^{-1} resolution, in a Thermo Nicolet IR300 Fourier transform infrared (FTIR) spectrometer, equipped with a Smart Orbit ATR accessory, a deuterated triglycine sulfate (DTGS) detector and a Ge/KBr beam splitter. The compound was then sublimated under high-vacuum conditions using a specially designed thermoelectrically heatable mini-oven placed inside the chamber of a cryogenic system (closed-cycle helium refrigerator APD Cryogenics, with a DE-202A expander). The sublimate was deposited onto the CsI optical cold substrate

of the cryostat ($T = 15 \pm 0.1$ K) to form a glassy state that was then probed by infrared spectroscopy, or isolated in an inert argon matrix by co-deposition of the sublimate with a large excess of argon (N60, Air Liquide) coming from a separate line. The obtained matrix was then subjected to infrared spectroscopy analysis. The details of the post-processing (temperature variation) of the samples obtained as described above are provided later in this article. The low-temperature IR spectra were registered, with 0.5 cm^{-1} resolution, using a Thermo Nicolet Nexus 670 FTIR spectrometer equipped with a DTGS detector and a Ge/KBr beam splitter, whose sample compartment was continuously purged by a flux of air free of H_2O vapor and CO_2.

Quantum chemical calculations

Quantum chemical calculations on tautomers **3** and **5** were performed using Gaussian 09 [17], at the density functional theory (DFT) level of theory, with the 6-311++G(d,p) basis set [18, 19] for all atoms except iodine, for which the LANL2DZ (Los Alamos National Laboratory 2 double-ζ) effective core potential (ECP) was used [20–22]. The DFT calculations were performed using the Becke 3-parameters, Lee, Yang and Parr (B3LYP) hybrid functional [23–25]. Calculated vibrational frequencies were obtained at the same level of approximation and subsequently scaled down by the factor 0.978, to account for the approximations inherent to the used theoretical model and anharmonicity [13].

Results and discussion

Synthesis

6-Methyl-7-iodo-4-oxo-quinoline-3-carboxylate (**6Me7I-EOQ, 3**) was synthesized from the α,β-unsaturated ester derivative **2** (Scheme 1, route a) by thermally driven intramolecular cyclisation, following the Gould-Jacobs methodology [10]. This 4-oxo-quinoline derivative (**3**) was characterized by mass spectrometry (provided as Supplementary Data – Fig. S7), elemental analysis and infrared spectroscopy, and its structure was investigated in detail through quantum chemistry calculations (see below). ^{1}H NMR and ^{13}C NMR data could not be obtained for compound **3** due to its poor solubility in all the available solvents. A previously described methodology [12] was adapted for the preparation of the enamine precursor **2** from diethyl ethoxymethylenemalonate and 3-iodo-4-methylaniline [10] which, in turn, was obtained from 2-iodo-4-nitrotoluene by reduction on the surface of metallic iron [26]. Mass, ^{1}H NMR and ^{13}C NMR spectra, of 3-iodo-4-methylaniline and of its enamine derivative **2**, are provided as Supplementary Data (Fig. S1–S6).

Considering the low solubility exhibited by 4-oxo-quinoline **3** it was decided to attempt the preparation of its 4-chloro-quinoline analog (**6Me7I-EClQ, 4**). Chloroquinolines are generally more soluble than the corresponding oxo derivatives, so chloroquinoline **4** would be more easily isolated and could then be converted into the corresponding 4-oxo-quinoline (Scheme 1, route c). Additionally, chloroquinolines are known as versatile building blocks [12]. We proposed that compound **4** would be a suitable intermediate for the preparation of quinolones with chemical diversity at position 7, given the versatility provided by the iodine substituent in this position (**4**; Scheme 1).

Although chloroquinoline **4** could be prepared directly from 4-oxo-quinoline **3** (Scheme 1, route b), we decided to attempt its synthesis from the α,β-unsaturated ester derivative **2** (Scheme 1, route d). This approach involves cyclisation of the enamine **2** and subsequent chlorination at position 4 of the quinolone core, in one pot, to afford the chloroquinoline **4** [11]. Application of the procedure outlined (Scheme 1, route d) and subsequent isolation afforded an amorphous solid corresponding to a sole compound. However, analysis by NMR spectroscopy and mass spectrometry provided data that were not compatible with the expected structure for chloroquinoline **4**. For example, by MS it was not possible to find a peak corresponding to the molecular ion (m/z 376 [$(M)^+$] or 399 [$(M+Na)^+$]) but, instead, a peak corresponding to m/z around 573 indicated the

presence of an unexpected product (MS spectrum provided as Supplementary Data – Fig. S8). It was then envisaged to proceed with characterization by X-ray crystallography. After crystallization, a suitable crystal was isolated and the crystal structure was investigated, revealing the presence of ethyl 7-iodo-4-(3-iodo-4-methylphenoxy)-6-methyl-quinoline-3-carboxylate (**6**, Scheme 2 and Fig. 2). The low isolated yield (12 %) presented for compound **6** may be due to difficulties on the nucleophilic attack by the 4-hydroxyl group in compound **5**, due to steric hindrance.

Crystal structure of ethyl 7-iodo-4-(3-iodo-4-methylphenoxy)-6-methyl-quinoline-3-carboxylate (6): The X-ray data obtained for compound **6** shows that the quinoline moiety is planar, with an rms deviation of the ring atoms from the least-squares plane of just 0.024 Å. The ethyl-carboxylate substituent is almost within the plane of the quinoline ring, the O2–C17–C3–C4 torsion angle being – 2.45°. The 3-iodo-methy-phenoxy substituent forms an angle of 59.62(13)° with the quinoline least-squares plane. There is some rotational flexibility of this substituent for rotations around the C4–O1 and O1–C11 bonds, as shown by the torsion angles C10–C4–O1–C11 and C4–O1–C11–C12 of 41.95 and 23.13°, respectively. It appears that such rotational flexibility might allow for the presence in the crystal of two alternate positions of this substituent, with occupancies of 96 % and 4 %, responsible for the presence of a small "ghost" peak of the iodine I2 atom in the alternate position corresponding to the minor disordered form.

Bond lengths and angles in the molecule are within the expected range of values. Packing of the molecules in the crystal appears to be dictated mainly by weak interactions between the π-clouds of the aromatic rings, resulting in a stacking of molecules along the *a*-axis (Fig. 3). In addition, there is a short C–H···Cg contact with the π-electron cloud of one of the aromatic rings.

The NMR and MS data previously obtained for compound **6** proved to be compatible with the structure obtained. The molecular weight of **6** (572.93 g/mol) fits in with the peak observed by mass spectrometry (MS spectrum as Supplementary Data – Fig. S8), m/z around 573. Also, the NMR spectra confirm the presence

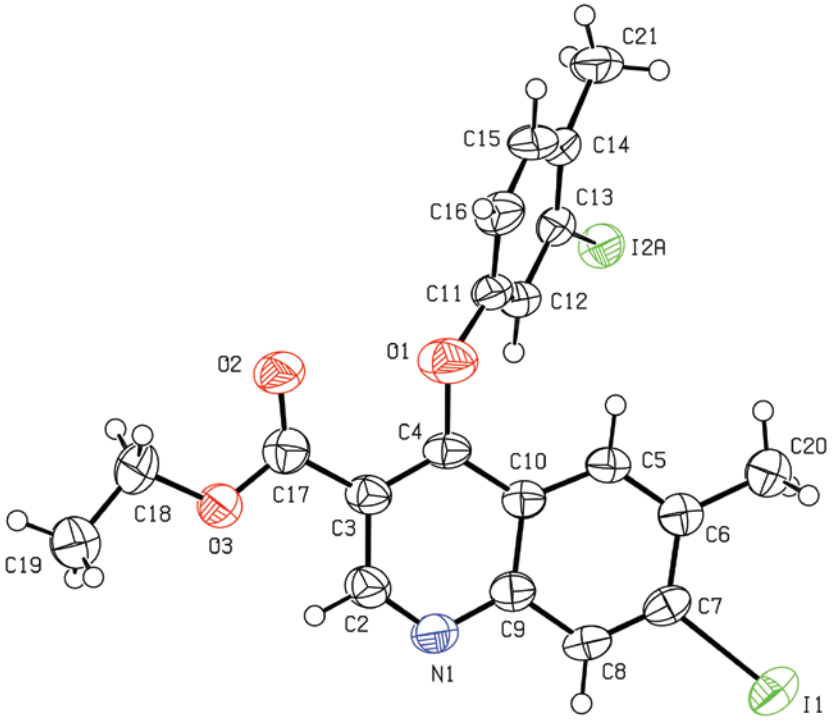

Fig. 2: ORTEP drawing with atom-labeling scheme of ethyl 7-iodo-4-(3-iodo-4-methylphenoxy)-6-methyl-quinoline-3-carboxylate (**6**) with thermal ellipsoids drawn at 50 % probability level. For clarity, the alternate position corresponding to the minor disordered form of the I2 atom is omitted.

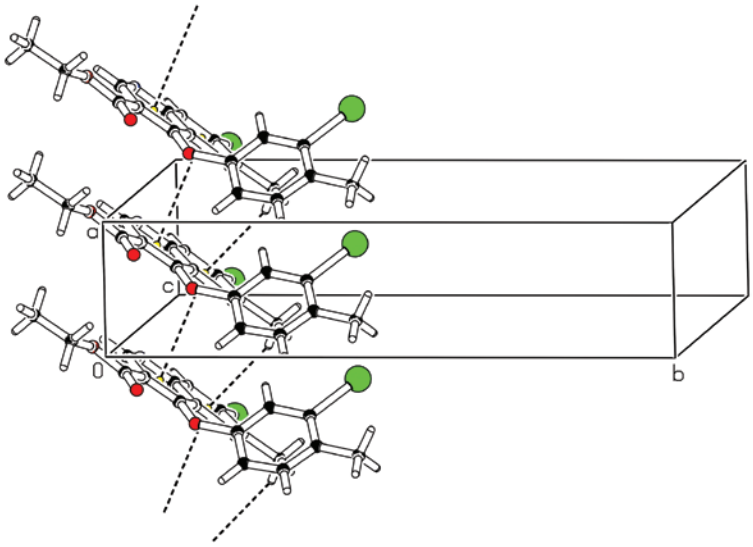

Fig. 3: Crystal packing of ethyl 7-iodo-4-(3-iodo-4-methylphenoxy)-6-methyl-quinoline-3-carboxylate (**6**) showing the network of Cg···Cg and C–H···Cg weak intermolecular interactions.

of structure **6** (Fig. S9 and S10 and Table S1 – Supplementary Data). Signals due to one additional aromatic ring, corresponding to resonances of the 4-aryloxy group (atom positions 11 to 16), are clearly observed in the ^{1}H NMR and in the ^{13}C NMR spectra. The presence of two methyl groups in compound **6** (atom positions 17 and 20) is also proved by the characteristic singlet peaks at 2.53 ppm and 2.37 ppm, in the ^{1}H NMR, and the peaks at 27.6 ppm and 26.8 ppm in the ^{13}C NMR spectra. Furthermore, it is important to note the absence of a signal due to the N–H group (present for oxo-quinoline compounds, but absent for **6**) and the presence of signals due solely to one ethyl ester group.

Isolation of the unexpected ether **6** raised some questions, and one of them is the mechanism underlying its synthesis. Our proposal, depicted in Scheme 2, considers initial formation of the 4-oxo-quinoline 3-ester **3**, as could be expected under the conditions outlined (Scheme 1, route d). The oxoquinoline may then undergo tautomerization to the corresponding 4-hydroxy-quinoline 3-ester **5**. Once formed, the hydroxy-quinoline tautomer **5** may act as nucleophile (through its 4-hydroxyl group), reacting with the enamine precursor **2** and subsequently affording the 4-aryloxyquinoline **6** (steric hindrance renders nucleophilic attack difficult, resulting in a low yield for the synthesis of compound **6**).

The quinolone/hydroxyquinoline tautomerism was previously observed for other quinolone 3-esters and has been investigated [13]. The relative amounts of both tautomeric forms depend mostly on the structure of both species and are also affected by the medium conditions. The mechanism proposed for the formation of ether **6** assumes the presence of a fair amount of 4-hydroxy-quinoline **5** in the reaction medium, this implicating that compound **5** is energetically favored, compared to its 4-oxo-quinoline tautomer **3**. To assess this aspect and gather more information to support a mechanistic proposal for the formation of ether **6**, we decided to proceed with a deeper investigation of the molecular structure of tautomers **3** and **5**, theoretically, using molecular orbital calculations, and experimentally, using matrix isolation coupled to FTIR spectroscopy.

Molecular structure of ethyl 4-oxo-6-methyl-7-iodo-quinoline-3-carboxylate (3) and its enol form (5): The 4-oxo-quinoline 3-ester **3** and its enol form, 4-hydroxy-quinoline **5**, were studied in more detail using infrared spectroscopy, complemented by quantum chemistry DFT calculations. The molecule of **3** has three conformationally flexible coordinates, defined by the torsions about the C–C bond connecting the ethyl carboxyester to the oxo-quinoline ring and the two C–O bonds (carboxylic and ester). It is well known [27, 28] that in carboxylic esters conformations with a *cis* arrangement (O=C–O–C dihedral ~0°) are by far more

stable than those having a *trans* (O=C–O–C dihedral ~ 180°) geometry. Keeping the *cis* arrangement about the C–O carboxylic bond, the performed DFT calculations yield four different conformers for the molecule of the oxo-quinoline **3**, with conformer **III** being the most stable form (Fig. 4).

Calculations performed at the same level of theory on the hydroxyquinoline tautomer **5**, which has one additional conformationally relevant torsion (defining the orientation of the OH group), revealed the existence, in this case, of eight different conformers with a *cis* arrangement about the C–O carboxylic bond. The two lowest energy forms (**I** and **II**) are stabilized by a strong O–H···O= intramolecular hydrogen bond and are considerably more stable than the remaining forms. The next two conformers of **5** in order of energy have a weaker intramolecular H-bond of type O–H···$O_{(ester)}$ (this type of H-bond is well-known to be weaker than the O–H···O= one because the carbonyl oxygen has a better ability to act as H-bond acceptor) [29, 30] and are more than 15 kJ mol^{-1} higher in energy than the most stable conformer **I** (Fig. 5). Very interestingly, the lowest energy conformers of the hydroxyquinoline **5** are lower in energy than the most stable conformer of its oxo-quinoline tautomer **3** by more than 27 kJ mol^{-1}. Such piece of information called for a detailed investigation on the nature of the tautomer (**3** or **5**) present in the synthesized solid sample through matrix isolation and FTIR spectroscopy studies.

Matrix-isolation and infrared spectroscopy studies: To obtain further insight on the **3**/**5** tautomerism, a series of experiments were designed. The first one was the collection of the infrared spectrum of the synthesized solid at room temperature. The examination of such spectrum, and its comparison with the calculated spectra for the more stable conformer of **3** and **5**, suggested the sole presence of the oxoquinoline tautomer in the sample. However, since in absolute terms the predicted spectra for the two tautomers have many similarities and also because the calculations were performed for the isolated molecules, so that the comparison of the calculated spectra with the experimental one for the solid sample could be expected a priori to have some limitations, we decided to obtain the infrared spectrum of the matrix-isolated species resulting from sublimation of the synthesized solid. Matrix isolation infrared spectroscopy is a very powerful technique for structure elucidation and is particularly sensitive to subtle structural modifications like those resulting from changes in conformation or tautomerization.

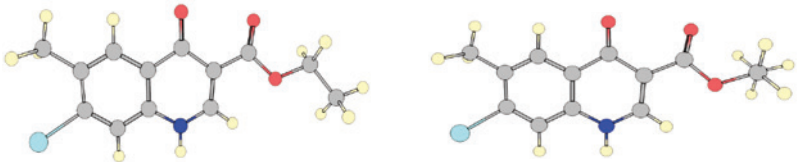

I (179.8, –165.9°)
8.2 [37.8]

II (86.0, –167.3°)
10.1 [39.7]

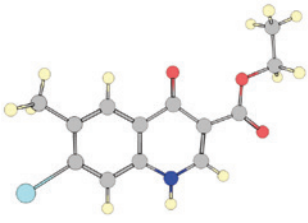

III (C_s)
0.0 [29.6]

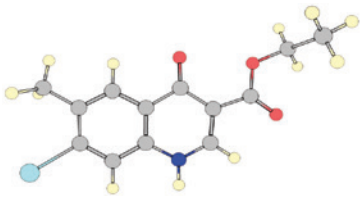

IV (86.9, 0.6°)
2.1 [31.7]

Fig. 4: B3LYP/6-311++G(d,p)/LANL2DZ optimized geometries for the 4 conformers of 6Me7I-EOQ (**3**) with a *cis* carboxylic-ester group (O=C–O–C ≈ 0°). Relative energies, in italic style, are in kJ mol^{-1} and are relative to the most stable conformer (**III**); the values in parentheses are relative to the most stable conformer of 6Me7I-EHQ (**5**). For conformers of C_1 symmetry, the C–O–C–C and C(O)–C–C–O dihedral angles are given, in this order, in parentheses. Note that all C_1 conformers shown in the figure have an equivalent-by-symmetry related form.

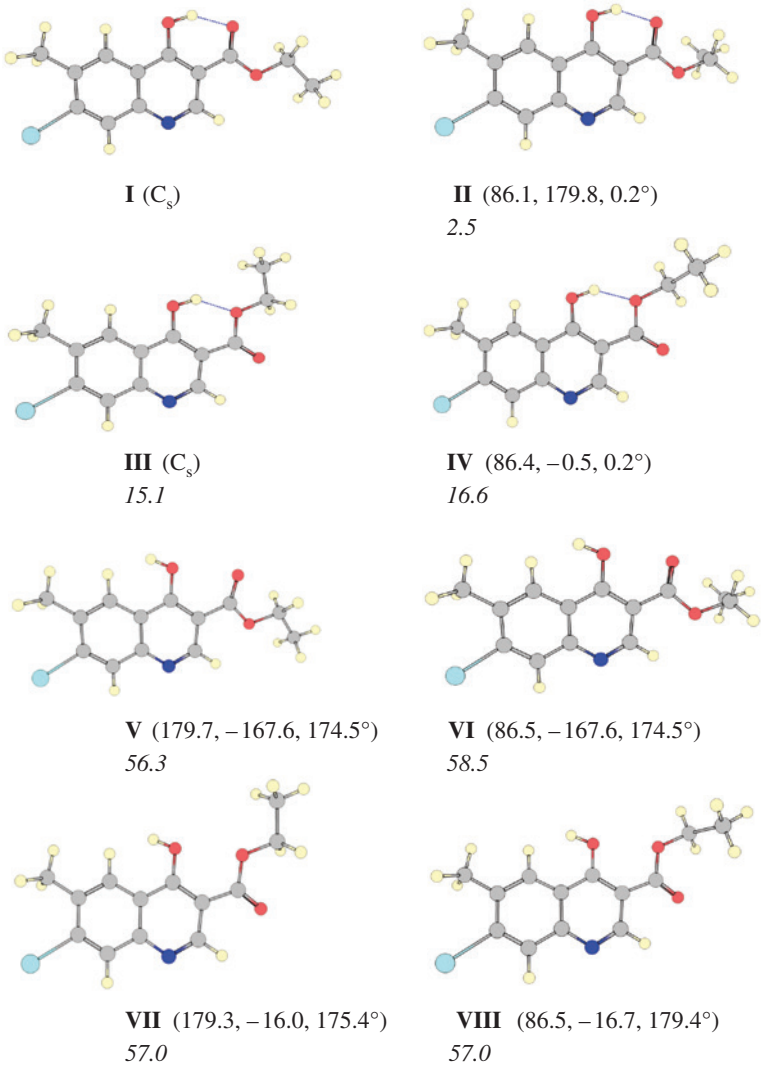

Fig. 5: B3LYP/6-311++G(d,p)/LANL2DZ optimized geometries for the eight conformers of 6Me7I-EHQ (**5**) with a *cis* carboxylic-ester group (O=C–O–C ≈ 0°). Relative energies, in italic style, are in kJ mol^{-1} and are relative to the most stable conformer (**I**). For conformers of C_1 symmetry, the C–O–C–C, C(OH)–C–C–O and C–C–O–H dihedral angles are given, in this order, in parentheses. Note that all C_1 conformers shown in the figure have an equivalent-by-symmetry related form.

The synthesized solid was then sublimated (at $T \sim 100$ °C) under high-vacuum, as described in the Section "Infrared spectroscopy studies", mixed with a large excess of argon, and deposited onto a CsI substrate cooled at 15 K, for IR spectra recording. The obtained spectrum is shown in Fig. 6, and fits very well the simulated spectrum for a mixture population of the two lowest energy conformers (**I** and **II**) of hydroxyquinoline **5** in the proportions expected to exist in the thermodynamic equilibrium at $T \sim 100$ °C (67 %: 33 %; ratio estimated considering the calculated relative energy of the two conformers and assuming the Boltzmann law). Moreover, annealing of the matrix up to 40 K led to changes in relative intensities which clearly reveal that upon increase of the temperature the less stable conformer **II** converts into the most stable form **I** (Fig. 7), as it could be anticipated considering that in a matrix isolation experiment the initially trapped conformers' populations are those existing in the vapor of the compound immediately before deposition (in this case those characteristic of the thermodynamic equilibrium at $T \sim 100$ °C) and should convert into those characteristic of the low temperature matrix (15 K) upon annealing of the matrix if the energy barrier separating the two conformers is low (as in the present case, where it amounts to ~ 2 kJ mol^{-1}; Fig. 8). The results of this experiment are then full consistent with the theoretical predictions, both in relation to the relative stability

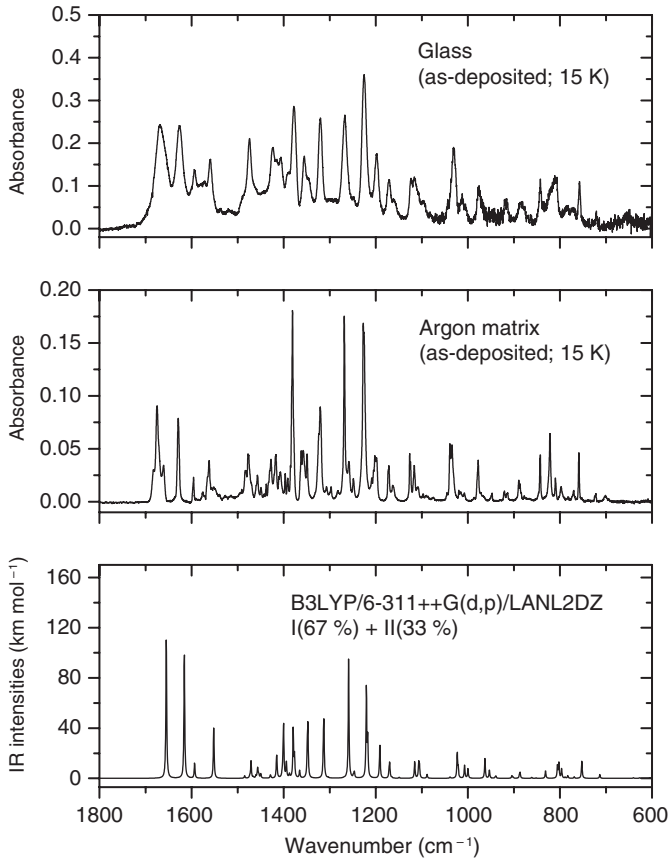

Fig. 6: Infrared spectra of (top): a glassy state resulting from deposition of vapors of the synthesized sample of 6Me7I-EOQ (**3**) onto an IR-transparent CsI windows mounted at the cold-tip of the cryostat (T=15 K); (middle): an argon matrix prepared by co-deposition of argon and vapors of the synthesized sample of 6Me7I-EOQ (**3**) onto an IR-transparent CsI windows mounted at the cold-tip of the cryostat (T=15 K); (bottom): simulated IR spectrum of a sample containing 67 % and 33 % of conformers **I** and **II** of 6Me7I-EHQ (**5**), built using the B3LYP/6-311++G(d,p)/LANL2DZ calculated IR spectra of these conformers with peaks broadened by convolution with Lorentzian functions centred at the calculated (scaled by 0.978) frequencies and peak areas equal to the calculated IR intensities. Sublimation of the 6Me7I-EOQ (**3**) crystal leads to conversion of the oxo-quinoline to the hydroxyl form (6Me7I-EHQ, **5**). (see text for detailed explanation).

of the two tautomers (**5** is in fact more stable than **3** in the gas-phase) and also in relation to the existence of two experimentally relevant low-energy conformers of the hydroxyquinoline **5**, with **I** being slightly more stable than **II**.

The next experiment consisted in preparing a sample in an identical way as used for the argon matrix preparation, but depositing just the vapor of the synthesized solid. In this case, we obtained a glassy state of the neat compound, since the fast deposition of the molecules present in the gas phase in the cold substrate precluded any molecular rearrangement to take place. The obtained spectrum of this sample is shown in Fig. 6, and it can clearly be seen from the comparison of this spectrum with that of the matrix-isolated species (the hydroxyquinoline **5**) that hydroxyquinoline **5** is the sole constituent in the low temperature glassy state prepared. The glassy state was then warmed stepwise, and at a temperature of about 115 K the spectrum starts to change. At 285 K the crystallization of the glass was complete (Fig. 9). The obtained spectrum of the crystal grown from the glass was found to be identical to that of the room temperature solid (Fig. 10), and the full set of data obtained in the described series of experiments doubtlessly indicated the sole presence of the oxoquinoline tautomer **3** in these samples.

In conclusion, in the gas phase the hydroxyquinoline tautomer **5** is the sole present species (in agreement with the much lower energy of the isolated molecule of this tautomer compared to that of **3**), while the crystalline phase is formed by the oxoquinoline **3** tautomer, as dictated by the crystal packing forces.

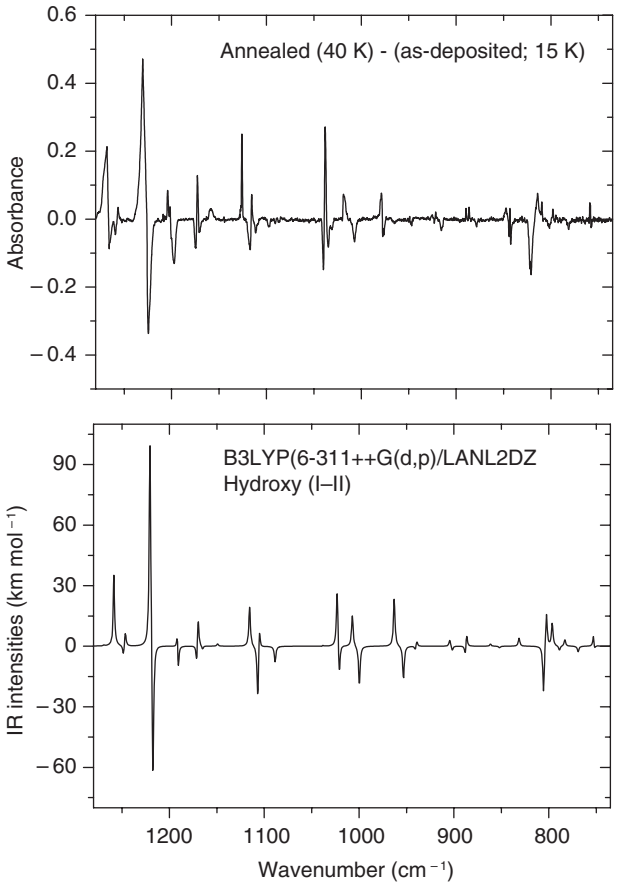

Fig. 7: Infrared difference spectra. (top): Annealed argon matrix (40 K) minus as-deposited matrix (15 K); (bottom): simulated IR difference spectrum (6Me7I-EHQ, **5**: **I** minus **II**), built using the B3LYP/6-311++G(d,p)/LANL2DZ calculated IR spectra of conformers **I** and **II** 6Me7I-EHQ (**5**) with peaks broadened by convolution with Lorentzian functions centred at the calculated (scaled by 0.978) frequencies and peak areas equal to the calculated IR intensities. Annealing of the matrix containing conformers **I** and **II** of 6Me7I-EHQ (**5**) at 40 K leads to the **II** → **I** conversion. (see text for detailed explanation).

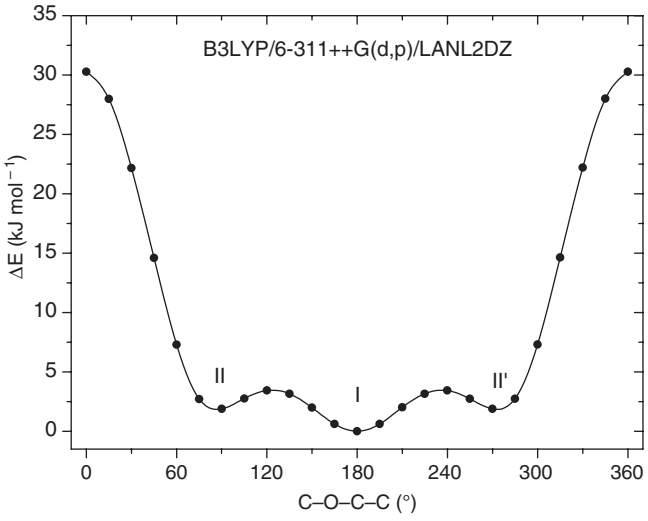

Fig. 8: Potential energy profile for rotation about the O–C ester bond leading to conformational interconversion between forms **I** and **II** of 6Me7I-EHQ (**5**).

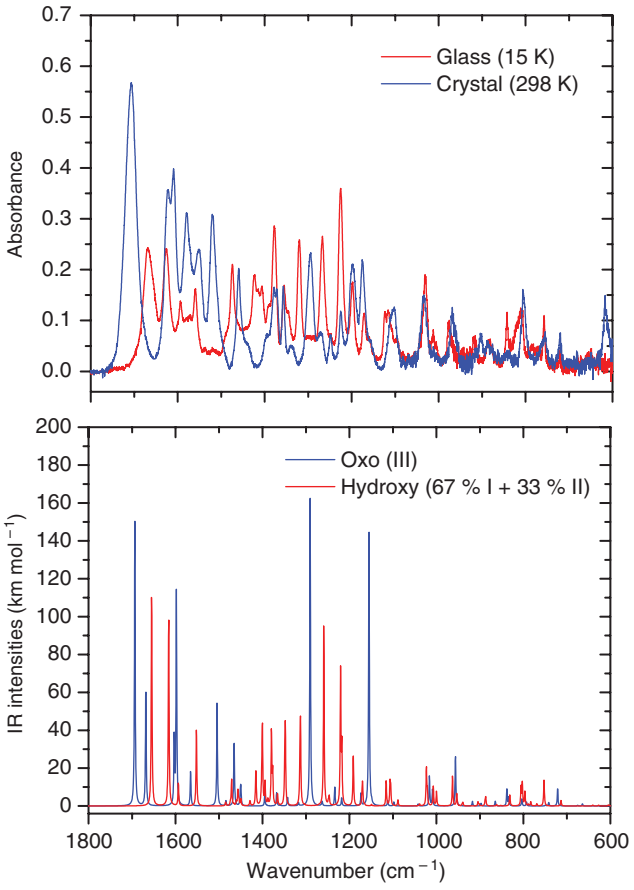

Fig. 9: Infrared spectra. (top): of the glassy state obtained by sublimation of vapors of the synthesized 6Me7I-EOQ (**3**) sample onto an IR-transparent CsI windows mounted at the cold-tip of the cryostat (T = 15 K) [red trace] and of the crystal resulting from warming of this glass [blue trace]; (bottom): simulated IR spectra of 6Me7I-EHQ (**5**) [red trace] and 6Me7I-EOQ (**3**) [blue trace], built using the B3LYP/6-311++G(d,p)/LANL2DZ calculated IR spectra of conformers **I** and **II** (67 %, 33 %, respectively) of 6Me7I-EHQ (**5**) and of conformer **III** of 6Me7I-EOQ (**3**), with peaks broadened by convolution with Lorentzian functions centred at the calculated (scaled by 0.978) frequencies and peak areas equal to the calculated IR intensities. Upon heating, the glassy state formed by 6Me7I-EHQ (**5**) gives rise to crystalline 6Me7I-EOQ (**3**) (crystallization starts to take place at ~ 115 K and is complete at 285 K).

Interestingly, though the intermolecular interactions are strong enough to induce the **5** → **3** tautomerization, the IR spectrum of the crystal is rather well reproduced by the theoretically calculated spectrum of the most stable monomer of **3**, indicating that the intramolecular vibrational potential is not very much perturbed by the intermolecular potential (see Fig. 10).

Although the 4-oxo-quinoline tautomer **3** is favored in the crystal phase, the results obtained from the structural studies point to a relatively easy tautomerization between 4-oxo-quinoline and 4-hydroxy-quinoline forms, compounds **3** and **5**, respectively. Thus, in the reaction conditions used (route d: $POCl_3$; 97 °C) a fair amount of the energetically more stable 4-hydroxy-quinoline tautomer **5** should be present in the reaction medium. It is worth noting that the reaction involves production of HCl as by-product, also favoring the production of the tautomer **5**, proposed as intermediate in the preparation of 4-aryloxy-quinoline derivative **6**.

The results obtained support our mechanistic proposal for the formation of the 4-aryloxy-quinoline derivative **6** through route d (Scheme 2) and re-enforce previous observations regarding the impact of the oxo/hydroxyquinoline tautomerization in the fate of available synthetic routes for the preparation of quinolones.

Biological activity and cLogP calculations: The 4-oxo-quinolone **3** and its 4-aryloxy-quinoline derivative **6** were evaluated in vitro for their antiplasmodial activity against two strains of *Plasmodium falciparum*:

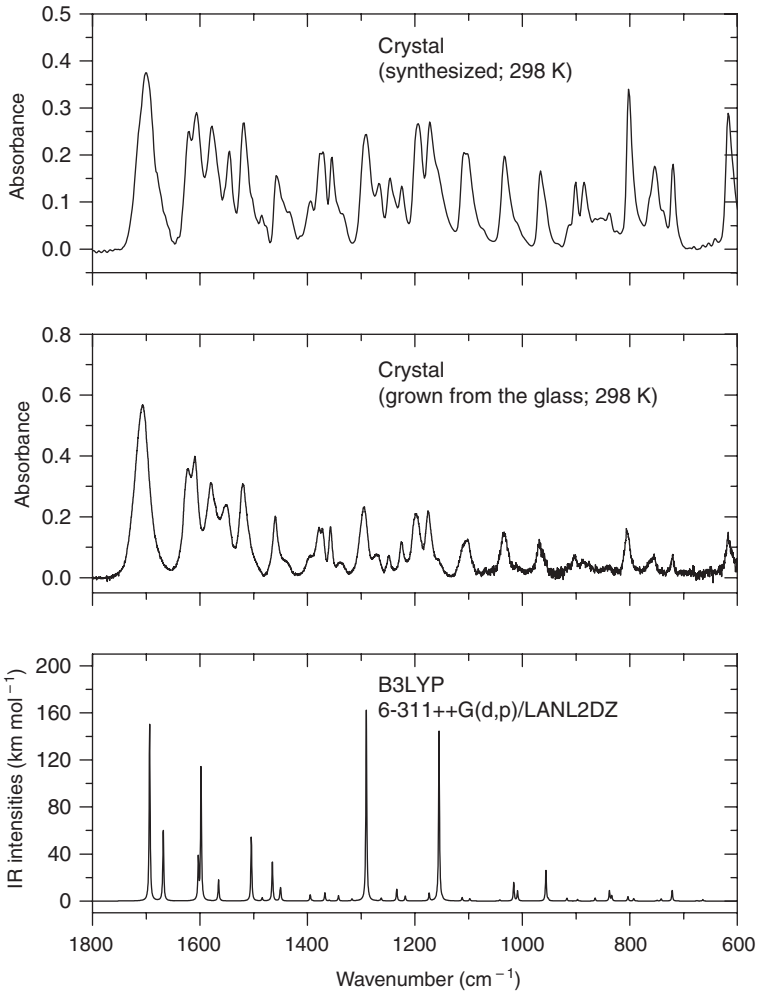

Fig. 10: Infrared spectra. (top): ATR IR spectrum of the synthesized 6Me7I-EOQ (**3**) sample; (middle): IR spectrum of the crystal (at 298 K) formed upon warming of the glassy state obtained by sublimation of vapors of the synthesized 6Me7I-EOQ (**3**) sample onto an IR-transparent CsI windows mounted at the cold-tip of the cryostat (T = 15 K); (bottom): simulated IR spectrum (6Me7I-EOQ, **3**), built using the B3LYP/6-311++G(d,p)/LANL2DZ calculated IR spectra of conformer **III** of 6Me7I-EOQ (**3**) with peaks broadened by convolution with Lorentzian functions centred at the calculated (scaled by 0.978) frequencies and peak areas equal to the calculated IR intensities. Upon heating, the glassy state formed by 6Me7I-EHQ (**5**) gives rise to crystalline 6Me7I-EOQ (**3**)-crystallization starts to take place at ~115 K and is complete at 285 K.

a sensitive (3D7) and a multiresistant strain (Dd2). As shown in Table 1, results of antiplasmodial activity against the strain 3D7, measured by IC_{50} values, fall in the high nanomolar range for both compounds, while for the multiresistant strain Dd2 the IC_{50} values increase to the low micromolar range. Also 4-oxo-quinoline

Table 1: cLogP for **6Me7I-EOQ** (**3**) and **6** and in vitro antimalarial activities.

Compound	cLogP[(a)] ± SD	Antiplasmodial activity (IC_{50}; μM) Average ± SD	
		3D7	Dd2
3	2.79 ± 0.37	0.323 ± 0.060	1.013 ± 0.088
6	6.18 ± 0.79	0.743 ± 0.124	1.553 ± 0.201

[a]by ALog PS2.1.

3 appears to be more active than its 4-aryloxy derivative, in both parasite models (e.g. IC_{50} values of 0.323 μM and 0.743 μM, respectively, against the strain 3D7).

In conclusion, both compounds are active against both CQ-sensitive and CQ-resistant malaria models. The better antimalarial activity demonstrated for compound **3**, compared to compound **6**, may be expected, considering the previous docking studies (importance of the N–H and 4-oxo groups in the quinolone core for enzyme inhibition). Thus, the 4-oxo-quinoline structure is expected to perform better from a pharmacodynamic viewpoint. Additionally, compound **6** presents a high cLogP value (6.18), which might mean that, as a drug, **6** is too hydrophobic and also too lipophilic. However, the possibility of easy 4-oxo-quinoline/4-hydroxy-quinoline tautomerization inside the enzyme pocket may impact in activity.

Supplementary data

Figures S1–S3, with the MS, ^{1}H NMR and ^{13}C NMR spectra of 3-iodo-4-methylaniline; Figs. S4–S6, with the MS, ^{1}H NMR and ^{13}C NMR spectra of diethyl 2-((3-iodo-4-methylaniline) methylene)malonate (**2**); Fig. S7, with the MS spectrum of ethyl 4-oxo-6-methyl-7-iodo-quinoline-3-carboxylate (**3**); Figs. S8–S10, with the MS, ^{1}H NMR and ^{13}C NMR spectra of ethyl 7-iodo-4-(3-iodo-4-methylphenoxy)-6-methyl-quinoline-3-carboxylate (**6**); and Table S1, with the observed ^{1}H-NMR and ^{13}C-NMR chemical shifts (δ; ppm) of ethyl 7-iodo-4-(3-iodo-4-methylphenoxy)-6-methyl-quinoline-3-carboxylate (**6**).

Acknowledgments: The authors gratefully acknowledge Fundação para a Ciência e Tecnologia (FCT – Portugal) for generous financial support: Project UID/Multi/04326/2013, cofunded by QREN-COMPETE-UE and CCMAR; P.H. acknowledges FCT for the award of a doctoral grant (SFRH/BD/81821/2011). NMR spectrometers used are part of The National NMR Facility, supported by FCT (RECI/BBB-BQB/0230/2012). R.F. and E.M.B. thank the funds made available to this research by the Project PTDC/QEQ-QFI/3284/2014 – POCI-01-0145-FEDER-016617. The Coimbra Chemistry Centre (CQC) is supported by FCT, through the project UI0313/QUI/2013, also co-funded by FEDER/COMPETE 2020-UE. The Coimbra Physics Centre (CFisUC) is supported by FCT, through the project UID/FIS/04564/2016.

References

[1] R. M. Beteck, F. J. Smit, R. K. Haynes, D. D. N'Da. *Malar. J.* **13**, 339 (2014).
[2] G. S. Bisacchi. *J. Med. Chem.* **58**, 4874 (2015).
[3] C. Sissi, M. Palumbo. *Curr. Med. Chem. Anticancer. Agents* **3**, 439 (2003).
[4] O. K. Kim, K. Ohemeng, J. F. Barrett. *Expert Opin. Investig. Drugs* **10**, 199 (2001).
[5] R. Cowley, S. Leung, N. Fisher, M. Al-Helal, N. G. Berry, A. S. Lawrenson, R. Sharma, A. E. Shone, S. A. Ward, G. A. Biagini, P. M. O'Neill. *Medchemcomm*. **3**, 39 (2012).
[6] "World Malaria Report 2014," World Health Organization, 2014.
[7] D. J. Hammond, J. R. Burchell, M. Pudney. *Mol. Biochem. Parasitol.* **14**, 97 (1985).
[8] H. J. Painter, J. M. Morrisey, M. W. Mather, A. B. Vaidya. *Nature* **446**, 88 (2007).
[9] G. A. Biagini, P. Viriyavejakul, P. M. O'Neill, P. G. Bray, S. A. Ward. *Antimicrob. Agents Chemother.* **50**, 1841 (2006).
[10] R. G. Gould, W. A. Jacobs. *J. Am. Chem. Soc.* **61**, 2890 (1939).
[11] A. K. Willard, R. L. Smith, E. J. Cragoe. *J. Org. Chem.* **46**, 3846 (1981).
[12] P. C. Horta, M. S. C. Henriques, N. Kuş, J. A. Paixão, P. M. O'Neill, M. L. S. Cristiano, R. Fausto. *Tetrahedron* **71**, 7583 (2015).
[13] P. Horta, N. Kuş, M. S. C. Henriques, J. A. Paixão, L. Coelho, F. Nogueira, P. M. O'Neill, R. Fausto, M. L. S. Cristiano. *J. Org. Chem.* **80**, 12244 (2015).
[14] "Bruker, APEX2, SAINT and SADABS," *Bruker AXS Inc.*, vol. Madison, W, 2006.
[15] G. M. Sheldrick. *Acta Crystallogr. Sect. A Found. Adv.* **71**(Pt 1), 3 (2015).
[16] G. M. Sheldrick. *Acta Crystallogr. Sect. C Struct. Chem.* **71**, 3 (2015).
[17] M. J. Frisch, G. W. Trucks, H. B. Schlegel, G. E. Scuseria, M. A. Robb, J. R. Cheeseman, G. Scalmani, V. Barone, B. Mennucci, G. A. Petersson, H. Nakatsuji, M. Caricato, X. Li, H. P. Hratchian, A. F. Izmaylov, J. Bloino, G. Zheng, J. L. Sonnenberg,

M. Hada, M. Ehara, K. Toyota, R. Fukuda, J. Hasegawa, M. Ishida, T. Nakajima, Y. Honda, O. Kitao, H. Nakai, T. Vreven, J. A. Montgomery, Jr., J. E. Peralta, F. Ogliaro, M. Bearpark, J. J. Heyd, E. Brothers, K. N. Kudin, V. N. Staroverov, R. Kobayashi, J. Normand, K. Raghavachari, A. Rendell, J. C. Burant, S. S. Iyengar, J. Tomasi, M. Cossi, N. Rega, J. M. Millam, M. Klene, J. E. Knox, J. B. Cross, V. Bakken, C. Adamo, J. Jaramillo, R. Gomperts, R. E. Stratmann, O. Yazyev, A. J. Austin, R. Cammi, C. Pomelli, J. W. Ochterski, R. L. Martin, K. Morokuma, V. G. Zakrzewski, G. A. Voth, P. Salvador, J. J. Dannenberg, S. Dapprich, A. D. Daniels, O. Farkas, J. B. Foresman, J. V. Ortiz, J. Cioslowski, D. J. Fox. *Gaussian 09, Revision A.02*. Gaussian, Inc., Wallingford, CT, 2009.

[18] A. D. McLean, G. S. Chandler. *J. Chem. Phys.* **72**, 5639 (1980).
[19] R. Krishnan, J. S. Binkley, R. Seeger, J. A. Pople. *J. Chem. Phys.* **72**, 650 (1980).
[20] T. H. Dunning. *J. Chem. Phys.* **90**, 1007 (1989).
[21] E. R. Davidson. *Chem. Phys. Lett.* **260**, 514 (1996).
[22] P. J. Hay, W. R. Wadt. *J. Chem. Phys.* **82**, 299 (1985).
[23] A. D. Becke. *Phys. Rev. A* **38**, 3098 (1988).
[24] C. Lee, W. Yang, R. G. Parr. *Phys. Rev. B* **37**, 785 (1988).
[25] S. H. Vosko, L. Wilk, M. Nusair. *Can. J. Phys.* **58**, 1200 (1980).
[26] I. Zilberberg, A. Pelmenschikov, C. J. Mcgrath, W. Davis, D. Leszczynska, J. Leszczynski. *Int. J. Mol. Sci.* **3**, 801 (2002).
[27] J. M. Riveros. *J. Chem. Phys.* **46**, 4605 (1967).
[28] D. G. Lister, N. L. Owen, P. Palmieri. *J. Mol. Struct.* **31**, 411 (1976).
[29] J. J. C. Teixeira-Dias, R. Fausto, L. A. E. B. de Carvalho. *J. Comput. Chem.* **12**, 1047 (1991).
[30] R. Fausto, L. A. E. B. de Carvalho, J. J. C. Teixeira-Dias, M. N. Ramos. *J. Chem. Soc. Faraday Trans. 2* **85**, 1945 (1989).

Supplemental Material: The online version of this article (DOI: 10.1515/pac-2016-1119) offers supplementary material, available to authorized users.